Predistortion of a radio frequency power amplifier

Ylva Jung

Division of Automatic Control

E-mail: ylvju@isy.liu.se

14th October 2010

Report no.: LiTH-ISY-R-2974

Address:
Department of Electrical Engineering
Linköpings universitet
SE-581 83 Linköping, Sweden

WWW: http://www.control.isy.liu.se

AUTOMATIC CONTROL
REGLERTEKNIK
LINKÖPINGS UNIVERSITET

Abstract

A linearized digital radio frequency (RF) power amplifier (PA), a switched RF PA, is more power efficient than an analog amplifier, but may cause interference in adjacent transmitting channels similar to analog amplifiers. This interference is due to the inherent nonlinearities, and this project investigated the possibility of reducing this interference by using a prefilter, a *predistorter*, to improve the linearity of the linearized digital amplifiers.

Two models, a forward model and an inverse model, the predistorter, have been estimated from measured data. The model addresses the gain and phase errors of the power amplifier. The first experiments show promising results, like improved Adjacent Channel Leakage Ratio (ACLR) for WCDMA and improved margins to the spectral mask for EDGE 8PSK measured at 2 GHz.

Predistortion of a radio frequency power amplifier

Ylva Jung – `ylvju@isy.liu.se`

2010-10-14

Abstract

A linearized digital radio frequency (RF) power amplifier (PA), a switched RF PA, is more power efficient than an analog amplifier, but may cause interference in adjacent transmitting channels similar to analog amplifiers. This interference is due to the inherent nonlinearities, and this project investigated the possibility of reducing this interference by using a prefilter, a *predistorter*, to improve the linearity of the linearized digital amplifiers.

Two models, a forward model and an inverse model, the predistorter, have been estimated from measured data. The model addresses the gain and phase errors of the power amplifier. The first experiments show promising results, like improved Adjacent Channel Leakage Ratio (ACLR) for WCDMA and improved margins to the spectral mask for EDGE 8PSK measured at 2 GHz.

1 Introduction

A linearized digital radio frequency (RF) power amplifier (PA), a switched RF PA, is more power efficient than an analog amplifier, but may cause interference in adjacent transmitting channels similar to analog amplifiers. This interference is due to the inherent nonlinearities, and the underlying idea of this project is to reduce this interference by using a prefilter, or a *predistorter*, in order to improve the linearity of the linearized digital amplifiers. Preferably, the predistorter should be the inverse of the amplifier, but since the PA (in general) is a dynamic nonlinear system, there might not be an exact inverse.

This report will begin with an introduction to the outphasing power amplifier in Section 2, followed by a description of the modeling in Section 3. The experimental setup and results are presented in Section 4 and the conclusions in Section 5. The results presented in this report are also described in [5].

2 The power amplifier

The power amplifier in this project is based on the outphasing concept, where an amplitude and phase modulated signal,

$$s(t) = r(t)e^{j\alpha(t)}; \quad 0 \le r(t) \le r_{max} \tag{1}$$

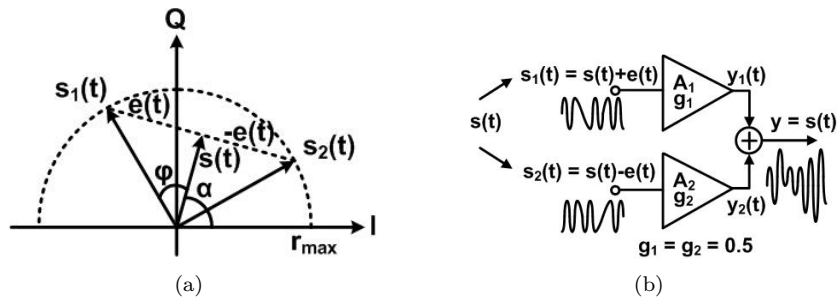is decomposed into two signals,

$$s_1(t) = s(t) + e(t) \tag{2}$$

Figure 1: (a) The decomposition of the original signal $s(t)$ into two constant amplitude signals $s_1(t)$ and $s_2(t)$ [4]. (b) Ideal power combining of the two constant-envelope signals.

and

$$s_2(t) = s(t) - e(t), \tag{3}$$

with constant amplitude, where $s_1(t), s_2(t) \in \mathbb{C}$. This is done using the original signal $s(t)$ and the quadrature signal

$$e(t) = js(t)\sqrt{\frac{r_{max}^2}{r^2(t)} - 1}, \tag{4}$$

see Figure 1(a).

The two constant amplitude signals are applied to two highly efficient nonlinear amplifiers, and the outputs are added in a power combiner, see Figure 1(b). In the power combiner, the quadrature signals cancel each other out and the output is an amplified version of the input signal $s(t)$. Perfect cancellation of the quadrature signals only takes place when the two PAs are balanced, otherwise the imbalance in phase or gain will lead to an incomplete cancellation of the quadrature signal, whose spectrum extends into neighbouring channels, causing interference [4].

3 Modeling

To better understand the PA, a model describing the connection between the input s and the output y has been estimated, referred to as the direct model, using estimation data. Then the inverse model, the digital predistortion (DPD) model was estimated, using the same data set. The DPD was applied to a second data set, validation data, that was evaluated on the PA.

The DPD was estimated in cascade with the PA model, as in Fig. 3(a), to assure that the *pre-inverse* is obtained, which is not necessarily the same as the post-inverse in the general case [6]. Also most system identification methods assume additive noise on the output [8], whereas an estimation of the post-inverse, from the output $y(t)$ to the input $s(t)$, would have the noise at the estimation input signal $y(t)$.
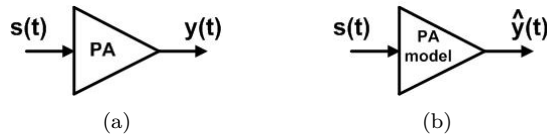
Figure 2: The notation and signals used for the real power amplifier (a), and the PA model (b).

3.1 Direct model

A forward model has been estimated from the measured input $s(t)$ and output $y(t)$ of the PA, see Figure 2. Since the signals $s_1(t)$ and $s_2(t)$ are amplified by two different amplifiers, there might be a small amplification difference resulting in a gain offset between these signals. A phase shift can also be thought of as a time delay, stemming from the fact that $s_1(t)$ and $s_2(t)$ take different routes to the power combiner. This results in a gain and phase offset in the PA. With this insight, a first model structure, Model structure A, is suggested as

$$y_A(t) = g_1 s_1(t + \delta) + g_2 s_2(t). \tag{5}$$

where g_1, g_2 and δ are real valued constants.

In the IQ plot (real part and imaginary part of a signal plotted against each other) of the output from the original amplified signal and the simulated output using model structure (5), the phase error appeared to be dependent on the amplitude of the input; the phase shift increases with an increasing input amplitude. As can be seen in Figure 1(a), the information about the amplitude of the original input signal $s(t)$ can also be found in the angle between $s_1(t)$ and $s_2(t)$,

$$\Delta_\psi(s_1, s_2) = \arg(s_1(t)) - \arg(s_2(t)) \tag{6}$$

(so $\Delta_\psi = 2\varphi$ in Figure 1(a)).

One way to model the amplitude dependent phase shift without changing the constant amplitude of signals $s_1(t)$ and $s_2(t)$ is to use a model structure with an exponential function with a polynomial of order n in the exponent, as

$$y_B(t) = g_1 s_1(t) e^{j\, p(\eta_1, \Delta_\psi(s_1, s_2))} + g_2 s_2(t) e^{j\, p(\eta_2, \Delta_\psi(s_1, s_2))} \tag{7}$$

where η_1 and η_2 are the vectors of polynomial coefficients in

$$p(\eta_k, \beta(s)) = \sum_{j=0}^{n} \eta_{k,j} \beta(s)^j \quad k = 1, 2, \tag{8}$$

and

$$\beta(s) = \Delta_\psi(s_1, s_2) \tag{9}$$

for this model structure, referred to as Model structure B.

Model structure B with the additional constraint $\eta_{1,i} = \eta_{2,i}, i = 1, 2, \ldots, n$ is referred to as Model structure C.

Another model was also investigated, where instead of using the phase difference of the input signals, $\Delta_\psi(s_1, s_2)$, the input amplitude $|s(t)|$ was used.

Table 1: Different model structures.

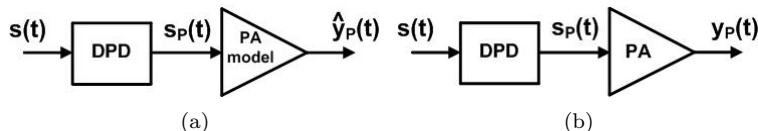| Model structure	$\beta(s)$	Linear coefficient	Nonlinear coeff.
A	$\Delta_\psi(s_1, s_2)$	different	none
B	$\Delta_\psi(s_1, s_2)$	different	different
C	$\Delta_\psi(s_1, s_2)$	different	same
D	$|s(t)|$	different	same

(a)   (b)

Figure 3: Estimation setup of the inverse model, the DPD, in (a), and intended use of the predistorter in (b).

This model structure is referred to as Model structure D. The different model structures are presented in Table 1.

The model parameters were estimated using a quadratic cost function as in

$$\hat{\theta} = \underset{\theta}{\arg\min} \sum_{t=1}^{N} \left| y(t) - \left(g_1 s_1(t) e^{j\, p(\eta_1, \beta(s))} + g_2 s_2(t) e^{j\, p(\eta_2, \beta(s))} \right) \right|^2 \quad (10)$$

where $\theta = [g_1 \quad g_2 \quad \eta_1^T \quad \eta_2^T]^T \in \mathbb{R}^{2n+4}$ and $y(t)$ is the measured data.

A more complex model structure has also been investigated by adding memory, that is to say that the output does not only depend on the current input but also previous inputs, as in the model structure

$$p_{mem}(\alpha, \bar{\beta}_{n_m}(s)) = \sum_{m=0}^{n_m} \sum_{j=0}^{n} \alpha_{mj} \beta(s(t-m))^j \quad (11)$$

with a memory depth n_m, where

$$\bar{\beta}_{n_m}(s) = \left(\beta\big(s(t-m)\big) \right)_{m=0}^{n_m}. \quad (12)$$

Another strategy tested is frequency weighting, as in [7], where a weighting function $W(\omega)$ is used. This is done to enhance the importance of the out-of-band properties, since they may not contribute very much to the minimization criterion because of the big difference in amplification between in-band and out-of-band frequencies. With the results of the nonweighted models being satisfying (see Section 4), it was not looked into further.

3.2   DPD model

The predistorter is estimated using the direct model, see Figure 3. This is done to assure we obtain the *pre-inverse*, which might not be the same as the post-inverse in the general case. When identifying the DPD model the model structure is assumed to be the same as for the direct model, motivated by Theorem 7.26 in [9].

The minimization criterion used is

$$\hat{\theta}_{\text{DPD}} = \underset{\theta_{\text{DPD}}}{\text{argmin}} \sum_{t=1}^{N} \left| s(t) - \underbrace{\left(\hat{g}_1 s_{1,\text{P}}(t) e^{j\, p(\hat{\eta}_1, \beta(s_\text{P}))} + \hat{g}_2 s_{2,\text{P}}(t) e^{j\, p(\hat{\eta}_2, \beta(s_\text{P}))} \right)}_{\hat{y}_\text{P}(t)} \right|^2 \tag{13}$$

where

$$s_{k,\text{P}}(t) = s_k(t) e^{i\, p(\eta_{k,\text{DPD}}, \beta(s))}, \quad k = 1, 2, \tag{14}$$

$$s_\text{P}(t) = \frac{s_{1,\text{P}}(t) + s_{2,\text{P}}(t)}{2}, \tag{15}$$

and $\theta_{\text{DPD}} = [\eta_{1,\text{DPD}}^T \quad \eta_{2,\text{DPD}}^T]^T \in \mathbb{R}^{2n+2}$.

The resulting $\hat{\theta}_{\text{DPD}}$ contains the DPD model parameters. With this vector the signals $s_{1,\text{P}}(t)$ and $s_{2,\text{P}}(t)$ were produced using the estimation input data and $s_{1,\text{val},\text{P}}(t)$ and $s_{2,\text{val},\text{P}}(t)$ were produced using the validation input data. These signals are entered into the direct model as well as the PA and the results are presented in Sections 4.2 and 4.3.

4 Experiments

The models were evaluated with measurements on the power amplifier.

4.1 Setup

The DPD is applied to the input signal $s(t)$, creating the predistorted input signal $s_\text{P}(t)$. This signal (or, rather $s_{1,\text{P}}(t)$ and $s_{2,\text{P}}(t)$) is then fed into the PA, and the resulting output is measured.

The developed model structures have been evaluated on different signal types: EDGE, WCDMA and LTE. Most of the models evaluated used $n = 5$, which seemed like a reasonable model complexity, but model reduction or increasing the model order has not been looked into yet.

Enhanced Data Rates for GSM Evolution (EDGE) is a mobile phone technology with higher bit rates than General Packet Radio Service (GPRS) [1]. Two different modulations have been evaluated, mainly 8PSK but also to a limited extent the 32QAM. The carrier frequency used is 2 GHz, and the bandwidth is 200 kHz. The identification data set contains $N_{id} = 40\,001$ samples and the validation data set $N_{val} = 80\,001$. These signals were repeated $K = 150$ times and measured, whereupon a mean is calculated. This is done to minimize the influence of measurement noise. The input sample frequency is $f_s = 8.67$ MHz and the output sampling frequency is $f_{s,out} = 4f_s$.

Wideband Code Division Multiple Access (WCDMA) is a third generation (3G) mobile phone technology, and is one of the 3G mobile communications standards [3]. The carrier frequency used is 2 GHz, and the bandwidth is 5 MHz. The identification and validation data sets contain $N = 153\,600$ samples, and the signals were repeated $K = 200$ times and measured. The sample frequency is $f_s = 61.44$ MHz.

Very limited tests have also been performed on the Long Term Evolution (LTE) signal, sometimes called 4G or 3.9G since it does not completely satisfy

the 4G requirements [10]. The bandwidth of the LTE signal is variable, and can be adjusted between 1 and 20 MHz.

The EDGE and WCDMA signals used are created as random signals with predefined characteristics.

Two test cases have been evaluated. A rough first trimming will be needed at the first use of the PA, and then the DPD will be able to handle the finetuning. In Test case 1 an optimally tuned PA is used, while for Test case 2 there was an added phase error of $3°$.

4.2 EDGE results

A spectral mask is a nonlinearity measure describing the amount of power that is allowed to be spread to adjacent frequencies [4]. The non predistorted power amplifier output is below the spectral mask at most frequencies, but the DPD manages to improve the margins to the mask.

The result of using Model B on Test case 2 is presented in Figures 4, 5 and 6. Figure 4 shows the measured amplitude of the original input $s(t)$ and the simulated output from the PA model using a predistorted input, $\hat{y}_P(t)$, which are very similar (as we hope they would be). Figure 5 shows the resulting error, $|s(t) - \hat{y}_P(t)|$. Figure 6 shows the spectra of the input $s(t)$, the original output $y(t)$ and the predistorted output $y_P(t)$ and the spectral mask, as well as the spectrum of the output when Model C is used, for comparison. Both models reduce the nonlinearities and improve the margins to the mask.

The model used is a model without memory with $n = 5$. This means that Model B uses 14 parameters in the direct model and 12 parameters in the DPD, whereas Model C uses 9 and 7 parameters, respectively. Since the EDGE signal has a rather small dynamic range and is a narrowband signal, it does not seem unreasonable that such a simple model works well.

4.3 WCDMA results

The same model structures were applied to a WCDMA signal, leading to surprisingly good results. With WCDMA being a more broadband signal than EDGE, the initial guess was that some memory effects might show up, complicating the model. Therefore a model structure with added memory as in (11) was tested, but did not lead to a significantly better result.

The results of using Model C on Test case 2 are presented in Figures 7, 8 and 9. Figure 7 shows the amplitude plot of the PA output (without memory) and Figure 8 shows the resulting error $|s(t) - \hat{y}_P(t)|$. The spectrum for a model with and without memory can be seen in Figure 9. As can be seen, the DPD clearly reduces the nonlinearities induced by the PA, but the memory does not have a significant effect. The model used has $n = 4$. This means that Model C with $m = 0$ uses 8 parameters in the direct model and 6 parameters in the DPD, whereas Model C with $m = 1$ uses 12 and 10 parameters, respectively.

The Adjacent Channel Leakage Ratio (ACLR) is a measure that, like the spectral mask for EDGE, describes the amount of power spread to neighbouring frequencies. The ACLR can be calculated by integrating the spectrum over a bandwidth of 3.84 MHz at $\pm l \cdot 5$ MHz ($l = 1, 2$) distance from the center
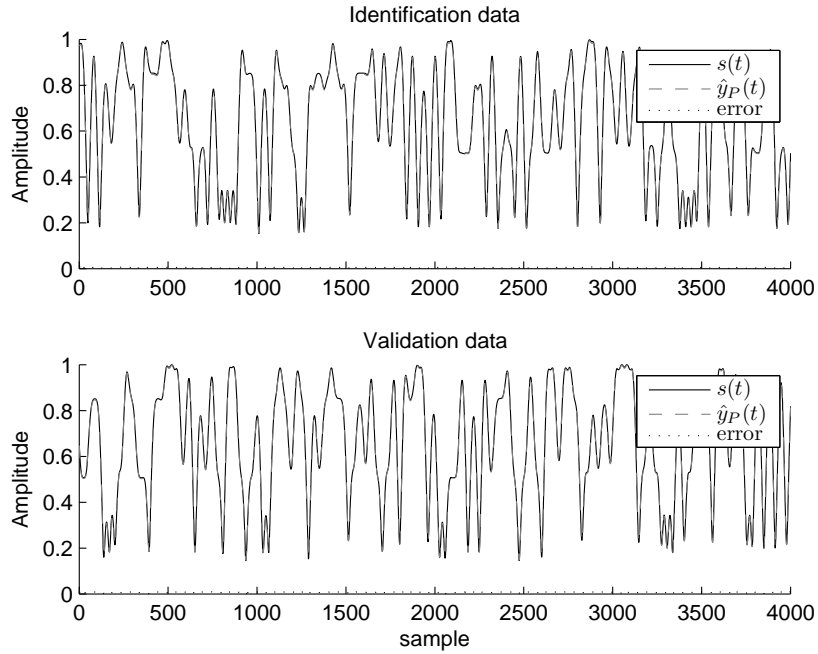
Figure 4: Amplitude plots of results using Model B on test case 2 with an EDGE input. The measured amplitude of the original input $s(t)$ and the simulated output from the PA model using a predistorted input, $\hat{y}_P(t)$. The two signals are almost identical. (a) shows the result for identification data and (b) for validation data.
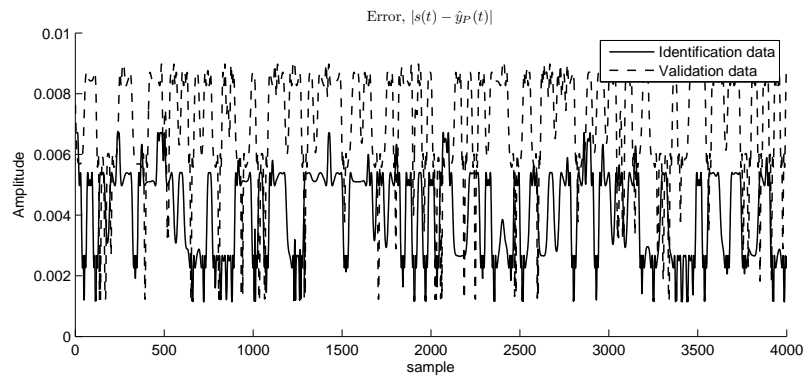

Figure 5: Amplitude plot of the error, $|s(t) - \hat{y}_P(t)|$, using Model B on test case 2, EDGE. As can be seen in Figure 4, the signals are very similar, and the resulting error is very small.

7
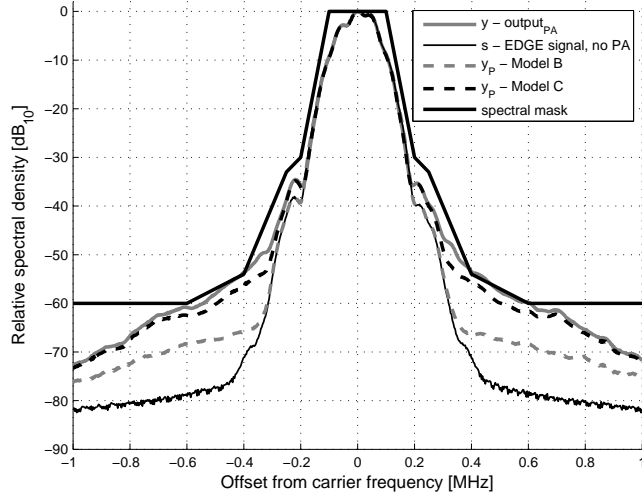
Figure 6: The spectral mask and the spectra of the original output $y(t)$, the input $s(t)$ and the predistorted outputs $y_P(t)$, using Models B and C on test case 2, EDGE.

frequency [2], as

$$\mathrm{ACLR} = \int_{l \cdot 5 - 1.92}^{l \cdot 5 + 1.92} \mathrm{WCDMA_{spectrum}} \, df, \quad l = \pm 1, \pm 2. \tag{16}$$

It can clearly be seen in Figure 9 that the ACLR will be improved at ± 5 MHz and roughly the same at ± 10 MHz.

5   Conclusions

The results from the first experiment show a significant improvement in performance for the EGDE 8PSK and WCDMA signals. For these signals a rather simple, static model sufficed. Added memory did not improve the predistorter performance.

The same model structures was tested on an EDGE 32QAM and an LTE signal, but did not manage to capture the PA behavior and there was not enough time to look into it further.
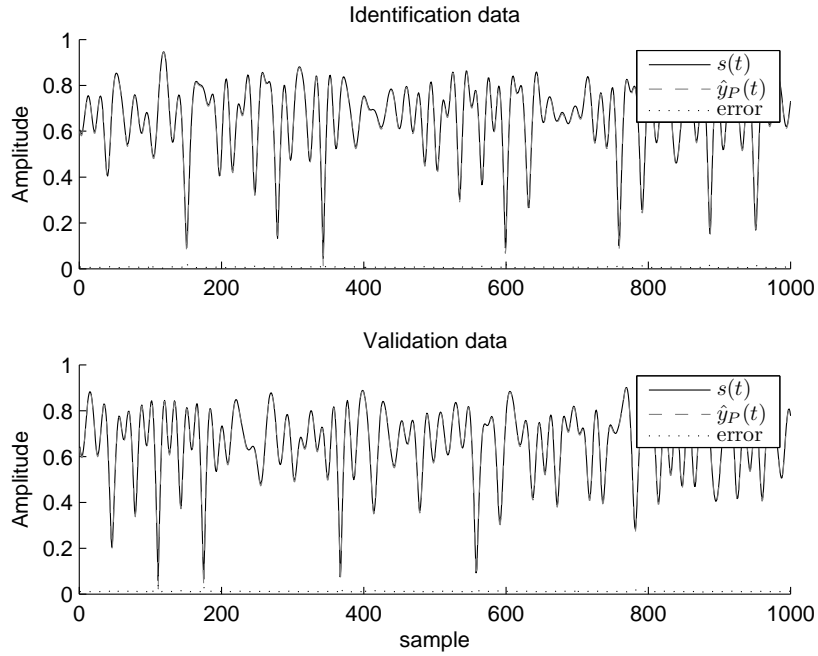
6   Acknowledgements

Figure 7: Amplitude plots of results using Model C on test case 2 with a WCDMA input, showing the measured amplitude of the original input $s(t)$ and the simulated output from the PA model using a predistorted input, $\hat{y}_P(t)$. (a) shows the result for identification data and (b) for validation data.
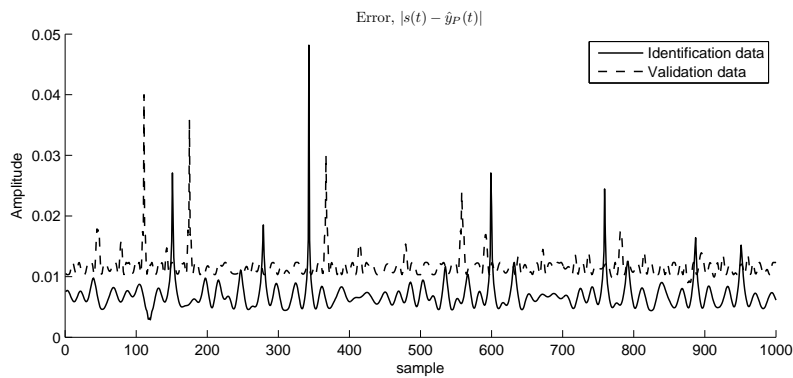

Figure 8: Amplitude plot of the error, $|s(t) - \hat{y}_P(t)|$, using Model C (without memory) on test case 2, WCDMA.
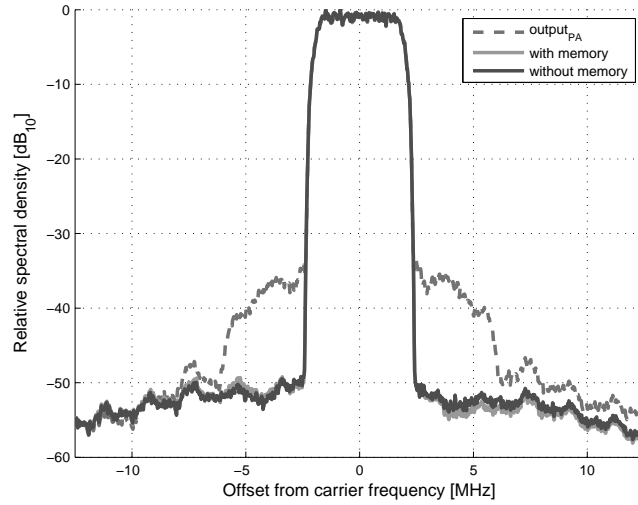
9

Figure 9: Spectral plot of the PA output without predistorsion, and predistorted outputs using a model without memory and with one memory term. The model structure used is Model C, on test case 2, WCDMA.

Abbreviations

The abbreviations used in the report can be found in Table 2.

Table 2: Abbreviations used in the report.

8PSK	Octonary-Phase-Shift Keying
32QAM	32-point quadrature amplitude modulation
ACLR	Adjacent Channel Leakage Ratio
DPD	Digital Predistortion
DLA	Direct Learning Architecture
EDGE	Enhanced Data Rates for GSM Evolution
GPRS	General Packet Radio Service
ILA	Indirect Learning Architecture
LTE	Long Term Evolution
NMSE	Normalized Mean Square Error
PA	Power Amplifier
RF	Radio Frequency
WCDMA	Wideband Code Division Multiple Access

References

[1] Lars Ahlin, Jens Zander, and Ben Slimane. *Principles of Wireless Communications.* Studentlitteratur, 2006.

[2] Anritsu. Adjacent Channel Power Ratio (ACPR), Application Note. `http://www.us.anritsu.com/downloads/files/11410-00264.pdf`. Accessed October 2010.

[3] Louis E. Frenzel. *Principles of Electronic Communication Systems*. McGraw Hill, third edition, 2007.

[4] Jonas Fritzin. Power amplifier circuits in CMOS technologies, 2009. LiU-TEK-LIC-2009:22. ISBN 978-91-7393-530-2.

[5] Jonas Fritzin, Ylva Jung, Per Niklas Landin, Peter Händel, Martin Enqvist, and Atila Alvandpour. Phase Predistortion of a Class-D Outphasing RF Amplifier in 90 nm CMOS. *Submitted to IEEE Transactions on Circuits and Systems II*, 2011.

[6] P. Kenington. *High-Linearity RF Amplifier Design*. Artech House, 2000.

[7] Per N. Landin, Magnus Isaksson, and Peter Händel. Parameter extraction and performance evaluation method for increased performance in RF power amplifier behavioral modeling. *International Journal of RF and Microwave Computer-Aided Engineering*, 20(2):200–208, March 2010.

[8] Lennart Ljung. *System Identification, Theory for the user*. Prentice Hall PTR, second edition, 1999.

[9] Walter Rudin. *Principles of Mathematical Analysis*. McGraw-Hill Book Co., third edition, 1976.

[10] Wikipedia. `http://en.wikipedia.org/wiki/3GPP_Long_Term_Evolution`, 2010-09-02.

Titel
Title

Predistortion of a radio frequency power amplifier

Författare
Author

Ylva Jung

Sammanfattning
Abstract

A linearized digital radio frequency (RF) power amplifier (PA), a switched RF PA, is more power efficient than an analog amplifier, but may cause interference in adjacent transmitting channels similar to analog amplifiers. This interference is due to the inherent nonlinearities, and this project investigated the possibility of reducing this interference by using a prefilter, a *predistorter*, to improve the linearity of the linearized digital amplifiers.

Two models, a forward model and an inverse model, the predistorter, have been estimated from measured data. The model addresses the gain and phase errors of the power amplifier. The first experiments show promising results, like improved Adjacent Channel Leakage Ratio (ACLR) for WCDMA and improved margins to the spectral mask for EDGE 8PSK measured at 2 GHz.